Efficient Numerical Simulation for Long Range Wave Propagation [1]

Kai Huang [2] George Papanicolaou [3] Knut Solna [2]

Chrysoula Tsogka [4] Hongkai Zhao [2]

[1]The research is partially supported by ONR Grant N00014-02-1-0090, DARPA Grant N00014-02-1-0603 and NSF Grant 0307011.

[2]Department of Mathematics, University of California at Irvine, CA 92697-3875

[3]Department of Mathematics, Stanford University, Stanford, CA 94305

[4]Department of Mathematics, University of Chicago, Chicago, IL 60637

Abstract

We develop an efficient algorithm for simulating wave propagation over long distances with both weak and strong scatterers. In domains with weak heterogeneities the wave field is decomposed into forward propagating and back scattered modes using two coupled parabolic equations. In the region near strong scatterers, the Helmholtz equation is used to capture the strong scattering events. The key idea in our method is to combine these two regimes using a combined domain decomposition and wave decomposition method. A transparent interface condition is derived to couple these two regions together. Numerical examples show that the simulated field is close to the field obtained using the full Helmholtz equation in the whole domain.

Keywords: Helmholtz equation, Parabolic approximation, Wave decomposition, Domain Decomposition.

1 Introduction

Wave propagation in complex media is a challenging multi-scale problem both mathematically and numerically. There are at least three typical length scales involved: the wave length, the propagation distance, and the correlation length (the scale on which the medium varies). These three scales can differ by several orders of magnitude. For example, in many applications, such as underwater acoustics, communications and remote sensing, the wave propagates over a long distance which can be several orders of magnitude larger than the wavelength. If the medium is inhomogeneous there is an additional characteristic scale corresponding to the correlation length of the medium inhomogeneities. If the wave length is much smaller than the correlation length of the medium, geometric optics provide in general a good approximation for the relatively smooth phase envelope. If the correlation length is much smaller than the wave length, homogenization theory gives an effective medium that can be used for propagation distances on the scale of the wavelength. Many wave propagation phenomena have a multi-scale nature in both space and time which complicates development of efficient numerical algorithms. In this paper we focus mainly on developing an efficient algorithm for the simulation of wave propagation in frequency domain. After Fourier transform in time the wave equation is reduced to the Helmholtz equation in space (for a fixed wave number), which is a boundary value problem. Due to the oscillatory wave nature of the solution, basic sampling conditions require resolution of the wavelength for numerical discretization. If the computational domain is large compared to the wave length, which corresponds to a large wave number, then the numerical discretization will result in a large system of equations. Moreover, unlike coercive elliptic equations, this discretized system is not positive definite. Computations are therefore very demanding both with respect

to CPU time and memory. Direct solvers are too costly due to memory constraints and iterative solvers may not converge or may converge slowly. However, if the wave propagates in a weakly inhomogeneous medium, e.g., underwater acoustics or electromagnetic waves in the atmosphere [12, 19, 22], the Helmholtz equation can be further simplified. In a situation where the propagation distance is much larger than the transverse dimension corresponding to a narrow angle geometry and when the back scattering can be neglected the Helmholtz equation can be reduced to a parabolic equation. The main advantage of the parabolic approximation is that it gives an initial value problem which is much easier to analyze and much cheaper to compute. The parabolic equation (PE) approximation provides an important tool for analysis and computation of wave propagation. Generalized parabolic approximations have been developed to deal with back scattering and wide angle geometries. For example the two way parabolic approximation by Collins [7], see also the review paper [11] for more detailed survey of the parabolic approximations. Strong scattering and/or multiple scattering events from scatterers of arbitrary geometry is still a challenge using parabolic approximations. In many applications, such as underwater acoustics and electromagnetic waves in the atmosphere, there are strong localized scatterers or targets embedded in the weakly heterogeneous background. In [13] Fishman developed a one-way propagation formulation based on wave-field decomposition and the scattering operators. The wave field is decomposed as $u = u^{(+)} + u^{(-)}$ and the condition $u_z = iB(z)[u^+ - u^{(-)}]$ is required, where z is propagation direction and $B(z) = \sqrt{\partial_x^2 + k^2(x,z)}$ is the square root operator which can be defined based on the eigenvalues and eigenfunctions of the transverse operator $\partial_x^2 + k^2$. The construction of several explicit, uniform asymptotic approximations of the square root Helmholtz operator are given in [14]. A re-formulation based on the Dirichlet-to-Neumann (DtN) map has also been derived in [16] and [17, 18]. An operator Riccati equation should be solved for decreasing propagating distance with an initial condition that matches the exact radiation condition at ∞. While the field should be solved for increasing propagating distance. This is practical only if the total number of operator

equation solutions required is not very large.

The key motivation in this paper is to couple parabolic approximation with full Helmholtz equation to deal with more general situations. Here we develop an approach based on both domain decomposition and wave field decomposition to deal with this situation with large propagation distances and short correlation length for the medium fluctuations. We decompose the wave propagation domain into two types of regions as illustrated in Figure 1. In the region of weak heterogeneities and long propagation distance, a coupled parabolic approximation is used, while in the region where there are strong scatterers, the Helmholtz equation is used.

There are two crucial steps involved in coupling the solution from these two regions consistently. First, we implement a boundary condition that is consistent with the wave field decomposition and is transparent to waves propagating in different directions at the interface between these two regions. We comment that our approach is different from the typical domain decomposition method since our computational domain is decomposed according to different physical regimes and different types of approximation are used in each sub-domain, moreover, since the boundary condition between the sub-domains is transparent to let information pass through rather than being absorbing [6] to damp the error propagation. Second, we decompose the wave field in the parabolic approximation region into two coupled parabolic equations to take into account both forward propagating waves and the back scattered wave due to the presence of the strong scattering in the Helmholtz region. The parabolic region has weak random medium fluctuations and is associated with long range propagation. The following coupled parabolic system is used as a correction of the standard parabolic equation approximation of the Helmholtz equation there:

$$\begin{aligned} 2ikA_z + \triangle_\perp A + k^2\nu A &= -k^2\nu B e^{-2ikz}, \\ -2ikB_z + \triangle_\perp B + k^2\nu B &= -k^2\nu A e^{2ikz}. \end{aligned} \tag{1}$$

This system derives from an approximation of the Helmholtz equation after expressing the wave field in terms of left and right (with respect to z) propagating modes.

In the layered case this system is exact and reads

$$\begin{aligned}\frac{\partial A}{\partial z} &= \frac{ik}{2}\nu\left(A + Be^{-2ikz}\right),\\ \frac{\partial B}{\partial z} &= \frac{ik}{2}\nu\left(Ae^{2ikz} + B\right),\end{aligned}$$

and is analyzed in for instance [1]. The random field ν corresponds to the random fluctuations in the refractive index. This system captures very strong longitudinal scattering and interaction of modes that is associated with a strongly fluctuating layered medium. In the case with a general three dimensional variation in the index of refraction, the two left hand sides in (1) gives the system

$$\begin{aligned}2ikA_z + \triangle_\perp A + k^2\nu A &= 0,\\ -2ikB_z + \triangle_\perp B + k^2\nu B &= 0,\end{aligned}$$

which are the standard parabolic equations with a random potential that describes long range (uncoupled) propagation in a fluctuating medium. They capture the effects of transversal scattering for these modes in the associated narrow angle geometry. Finally, observe that in the deterministic case $\nu = 0$ the system (1) becomes

$$\begin{aligned}2ikA_z + \triangle_\perp A &= 0,\\ -2ikB_z + \triangle_\perp B &= 0,\end{aligned}$$

which are the leading order transport equations of geometrical optics that are associated with a left or right outgoing condition for high frequency waves and captures geometrical spreading effects. The system (1) can be generalized to the situation with a slowly varying background and then include a phase term that comes from the solution of the Eiconal equation, see (9) below.

The outline of our paper is as follows. In Section 2 we describe the general setup of the problem and the main approach. In section 3 we derive the wave-field decomposition for the parabolic approximation and the transparent boundary condition between sub-domains. Numerical implementations and numerical examples are presented in section 4. A stability analysis for the wave decomposition is given in Appendix A.

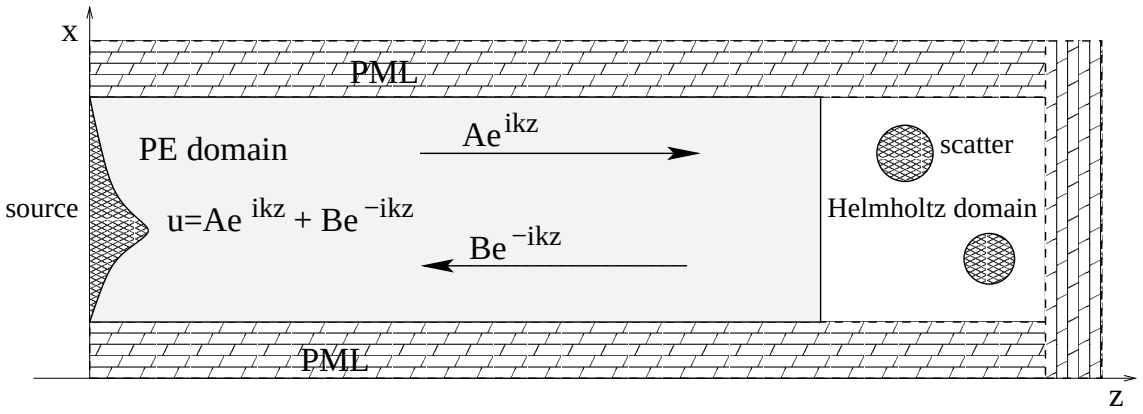

Figure 1: P-H domain decomposition

2 The Basic Setup and Wave Decomposition

We consider propagation of acoustic waves over long distances in weakly heterogeneous background with localized strong scatterers. Let $\mathbf{u}(\mathbf{x},t)$ and $p(\mathbf{x},t)$ be the acoustic velocity and pressure satisfying the equation of continuity of momentum and mass

$$\rho \mathbf{u}_t + \nabla p = \mathbf{F}(\mathbf{x},t)\,, \tag{2}$$

$$K^{-1} p_t + \nabla \cdot \mathbf{u} = 0, \tag{3}$$

where t is time, z is depth into the medium and defined so as to increase with depth, $(\mathbf{x},z) = (x,y,z)$ are the space coordinates, ρ is the density, K is bulk modulus, and the source is $\mathbf{F}(\mathbf{x},\mathrm{t})$. We model the medium by $\rho = \rho_0$ constant and

$$K^{-1}(\mathbf{x},z) = \begin{cases} K_0^{-1} & z \in (-\infty, 0] \\ K_p^{-1}(\mathbf{x},z)(1+\nu(\mathbf{x},z)) & z \in (0,\infty). \end{cases}$$

The function ν modulating the compliance corresponds to the medium fluctuations. In the case of a stationary random medium it is a zero-mean, stationary stochastic process whose statistics take on particular forms depending on the assumptions about the medium, whether it is locally layered, strongly or weakly heterogeneous media and so on [1]. In our discussion here ν models the weak medium

heterogeneities. At this stage, the source term is omitted, but it will be taken into account through the initial conditions for the parabolic equation.

Eliminating $\mathbf{u}$ from equations (2) and (3), we get

$$\triangle p - \frac{\rho}{K} p_{tt} = 0. \tag{4}$$

The time-harmonic version of (4) is the Helmholtz Equation:

$$\triangle \hat{p} + (1+\nu)\omega^2 \gamma^2 \hat{p} = 0\,, \tag{5}$$

where

$$\gamma(\mathbf{x}, z) = \sqrt{K_p^{-1}(\mathbf{x}, z)\rho}\,,$$

and $\hat{p}$ is the Fourier transform of p with respect to time:

$$\hat{p} \;\; = \;\; \int p e^{i\omega t}\, dt.$$

Note that below we suppress the 'hat' and that γ represents the effective slowness and $1/\gamma$ the speed in the corresponding effective medium.

The Helmholtz equation is a boundary value problem. If the computational domain is large compared to the wavelength, solving the discretized linear system using a direct method may be impossible due to memory constraints. Moreover, since the linear system is not positive definite, usual iterative methods typically converge slowly, if at all. We propose a domain decomposition approach by dividing the whole domain into two types of sub-domains, as is illustrated in Figure 1. The wave propagates over a long distance and in a weakly heterogeneous medium in the first type of sub-domain, in the second type of sub-domains there are strong scatterers present.

In the first type of sub-domains the parabolic approximation can be used to simulate the wave propagation. The basic approach is to neglect the back scattering, and only consider waves going mainly in one direction, as the medium is only weakly heterogeneous and the domain fits into a narrow angle geometry. The

parabolic approximation becomes an initial value problem which significantly reduces the complexity for both analysis and computation. This approximation is accurate in many scenarios such as in range dependent ocean wave-guides or in the case of atmospheric wave propagation. However in our setup, although there is no strong back scattering for wave propagation in the weakly heterogeneous domain, we need to capture the back scattered wave field from the domain that includes strong scatterers. Here we use a pair of coupled parabolic equations based on a wave-field decomposition formulation developed in [15, 21]. In fact, this coupled parabolic formulation also allows us to capture the effects of strong heterogeneities with slow lateral variations in the parabolic domain as was demonstrated in [15]. In the second type of sub-domains, the full Helmholtz equation has to be solved in the near field of strong scattering events. At the interface between these two type of domains appropriate boundary conditions have to be imposed, which allow the correct information to propagate through the interface. The crucial point in our formulation is that the wave-field decomposition in the parabolic domain is consistent with our transparent boundary condition at the interface.

In the following we first briefly review the wave decomposition and the coupled parabolic equations in the weakly heterogeneous domain. Then we describe the transparent boundary conditions and the domain decomposition algorithm.

2.1 Wave Decomposition and Coupled Parabolic Equations

In the standard parabolic approximation, assuming the wave is propagating along the positive z axis, the plane wave ansatz

$$p(\mathbf{x}, z) = A(\mathbf{x}, z) \exp(ik_0 z)\,, \tag{6}$$

can be used for the solution of Helmholtz equation:

$$\triangle p + \omega^2 \gamma^2(\mathbf{x}, z)(1 + \nu)p = 0\,, \tag{7}$$

where $k_0 = \omega/c_0$ is a reference wave number and $c_0 = \sqrt{K_p/\rho}$ is the background velocity. The factor $\exp(ik_0 z)$ in (6) represents a plane wave traveling in the positive z direction and is supposed to take out the rapid oscillations of p in the z direction; the function $A(\mathbf{x}, z)$ captures the modulation of the plane wave phase and usually varies slowly with z.

Substitution of Equation (6) into Equation (7) gives

$$\frac{\partial^2 A}{\partial z^2} + 2ik_0 \frac{\partial A}{\partial z} + \triangle_\perp A + [\omega^2\gamma^2(1+\nu) - k_0^2]A = 0\,, \tag{8}$$

with $\triangle_\perp$ being the Laplacian in the lateral coordinates $\mathbf{x}$. We next make the crucial paraxial approximation (small angle approximation) corresponding to the situation with

$$\frac{\partial^2 A}{\partial z^2} << 2ik_0 \frac{\partial A}{\partial z}\,,$$

so that we have

$$2ik_0 \frac{\partial A}{\partial z} + \triangle_\perp A + [\omega^2\gamma^2(1+\nu) - k_0^2]A = 0.$$

This approximation requires that we consider wave propagation in a narrow beam geometry, not close to the source and that the medium is weakly inhomogeneous. The resulting equation is called the narrow-angle parabolic equation (PE). In the PE method we take into account only waves traveling in the positive z direction; back scattering is neglected, see [12, 19].

Now we consider a more general wave decomposition. We define

$$\tau(z) = \int_{z_s}^{z} \sqrt{\frac{\rho}{K_p} - |\kappa|^2}\, ds = (z - z_s)\sqrt{\gamma^2 - |\kappa|^2}\,, \quad \text{and} \quad S^{\pm} = \kappa \cdot \mathbf{x} \pm \tau\,,$$

with κ being the lateral slowness vector. Note that S^+ is a plane wave phase corresponding to waves traveling in the spatial direction $(\kappa, \sqrt{\gamma^2 - |\kappa|^2})$. In the case with a general three dimensional background the phase terms $S^{\pm}$ will be solutions of the Eiconal equation associated with the slowness $\gamma(\mathbf{x}, z)$, see [1, 20, 21].

We decompose the wave into forward and backward modes :

$$\begin{aligned} p &= Ae^{i\omega S^+} + Be^{i\omega S^-}\,, \\ 0 &= A_z e^{i\omega S^+} + B_z e^{i\omega S^-}\,. \end{aligned}$$

Note that this plane wave decomposition is exact in the case of a homogenous medium and in the effective medium case when the effective medium parameters are constant.

Plugging this decomposition into the Helmholtz equation we get the following mode coupling transport equations:

$$\begin{aligned} 2\nabla S^+ \cdot \nabla A + \triangle S^+ A - i\omega\gamma^2\nu(A + Be^{i\omega(S^- - S^+)}) \\ = \frac{i}{\omega}\triangle_\perp A - R^- e^{i\omega(S^- - S^+)}\,, \end{aligned} \tag{9}$$

$$\begin{aligned} 2\nabla S^- \cdot \nabla B + \triangle S^- B - i\omega\gamma^2\nu(B + Ae^{i\omega(S^+ - S^-)}) \\ = \frac{i}{\omega}\triangle_\perp B - R^+ e^{i\omega(S^+ - S^-)}\,, \end{aligned} \tag{10}$$

with

$$\begin{aligned} R^+ &= 2\nabla_\perp S^+ \cdot \nabla_\perp A + \triangle S^+ A - \frac{i}{\omega}\triangle_\perp A\,, \\ R^- &= 2\nabla_\perp S^- \cdot \nabla_\perp B + \triangle S^- B - \frac{i}{\omega}\triangle_\perp B\,, \end{aligned}$$

where $\triangle_\perp$ is the transverse Laplacian. In the case that the fluctuations and the reflected field vanish, ($\nu \equiv 0, B \equiv 0$), (9) becomes

$$2\nabla S^+ \cdot \nabla A + \triangle S^+ A = \frac{i}{\omega}\triangle_\perp A\,,$$

which in the high frequency limit gives

$$2\nabla S^+ \cdot \nabla A_0 + \triangle S^+ A_0 = 0\,,$$

that is, the leading order transport equation of geometrical optics.

Here, we will consider the generalization of the parabolic case with waves propagating primarily in the z direction and set $\kappa = 0$. Then the coupling transport equations become

$$2ikA_z + \triangle_\perp A + k^2\nu A = -(k^2\nu B + \triangle_\perp B)e^{-2ikz}\,, \tag{11}$$

$$-2ikB_z + \triangle_\perp B + k^2\nu B = -(k^2\nu A + \triangle_\perp A)e^{2ikz}\,, \tag{12}$$

with $k = \gamma\omega$. A particular κ corresponds to a specific plane wave mode. This variable is the Fourier variable dual to the lateral space variable $\mathbf{x}$ introduced when the wave field in space and time is transformed into plane wave modes via Fourier transformation with respect to the lateral spatial coordinates. We next continue our discussion of the system (11) and (12) by introducing specific boundary conditions and a scheme for numerical approximation of the solution.

A naive Jacobi iteration of these coupled parabolic equations corresponds to solving for A using the current B in a source term and then solving for B with current A defining a source term and then iterate. This would reduce the computation of the Helmholtz equation into the computation of a sequence of parabolic equations. However, as we show in Appendix A, this iterative procedure is not stable. That is, without solving for A and B simultaneously evanescent modes will grow exponentially, with the instability caused by the coupling transverse Laplacian.

Since we are interested in the narrow angle wave propagation in the z-direction and long distance propagation, we drop the lateral scattering terms $\triangle_\perp B$ (respectively $\triangle_\perp A$) when we solve for $A(x,z)$ (respectively $B(x,z)$) in (11) (respectively (12)). Consider the equation (11). In the homogeneous case with $\nu \equiv 0$ the terms involving the reflected field B will be lower order correction terms to the paraxial approximation. We will consider regimes where there is significant back-scattering due to the scatterer ν and therefore retain the term involving ν in the coupling part of equations (11) and (12):

$$2ikA_z + \triangle_\perp A + k^2\nu A = -k^2\nu B e^{-2ikz}\,, \tag{13}$$

$$-2ikB_z + \triangle_\perp B + k^2\nu B = -k^2\nu A e^{2ikz}. \quad (14)$$

3 P-H Domain Decomposition and the Interface Condition

The two reduced coupled parabolic equations can simulate wave propagation over long distances. Both the forward propagating field and backward propagating field as well as their interactions are captured. The domain will be decomposed into parabolic region Ω_P and Helmholtz region Ω_H as shown in Figure 1 and we design transparent boundary conditions consistent with our wave decomposition to couple the wave fields in these two regions together. From the wave decomposition

$$\begin{aligned} u &= Ae^{ikz} + Be^{-ikz}, \\ 0 &= A_z e^{ikz} + B_z e^{-ikz}, \end{aligned}$$

we find

$$iku + u_z = 2ikAe^{ikz}, \quad (15)$$

$$B = \frac{iku - u_z}{2ik} e^{ikz}. \quad (16)$$

After solving the parabolic equation (13), we use (15) as the boundary condition when solving the Helmholtz equation in Ω_H, and then we use (16) as the initial condition for solving the parabolic equation (14) in Ω_P, i.e., the incoming wave is passed from parabolic region to the Helmholtz region and the back scattered wave is passed correspondingly.

3.1 Initial Condition For the Parabolic Equation

We assume that the scatterer ν is compactly supported and is located in a slab of thickness L, so that k is constant for $z < 0$ and $z > L$. The source is located in the homogeneous medium, at $z_s < 0$. Recall that with $B = 0$ the amplitude equation for

A is equivalent to the standard parabolic equation. We impose an initial condition for the total field u at $z = 0$. We use a Gaussian form for the initial data [22]:

$$u(\mathbf{x}, 0) = \sqrt{k_0} e^{-\frac{|\mathbf{x}|^2}{2}}.$$

Consequently, the initial data for A is

$$A(\mathbf{x}, 0) = u(\mathbf{x}, 0) - B(\mathbf{x}, 0).$$

3.2 Artificial Boundary Condition

The governing wave equation

$$-\triangle u - \omega^2 u = f \quad \text{in } \mathbf{R}^d\,, \tag{17}$$

$$\lim_{r\to\infty} r^{(d-1)/2}(\frac{\partial u}{\partial r} - i\omega u) = 0\,, \tag{18}$$

describes linear propagation of time-harmonic acoustic waves. The Sommerfeld radiation condition (18) states that the solution u is outgoing at infinity. The finite-element or finite-difference solution of this problem requires the unbounded domain to be truncated at a finite distance, and it becomes necessary to approximate the radiation condition at the truncation boundary. We truncate the domain by adding a PML (Perfectly Matched Layer) artificial boundary.

The idea is to introduce an exterior layer at the artificial boundary in such a way that all plane waves are totally absorbed, and no reflection occurs at the boundary [4]. For simplicity, we assume two spatial dimensions corresponding to one lateral dimension. In order to introduce the artificial boundary condition we return to the Helmholtz equation:

$$p_{zz} + p_{xx} + k^2(1 + \nu(x, z))p = 0.$$

In the matched layer we change this equation to obtain damping of the plane wave modes. We introduce the governing equations

$$\frac{\partial^2 p}{\partial z^2} + \frac{i\omega}{\sigma_1 - i\omega}\frac{\partial}{\partial x}\left(\frac{i\omega}{\sigma_1 - i\omega}\frac{\partial p}{\partial x}\right) + k^2(1+\nu)p \;=\; 0\,,$$

where $\sigma_1 > 0$ in the artificial domain giving damping of the plane wave modes, whereas $\sigma_1 = 0$ in the physical domain giving the Helmholtz equation there.

At the end of the slab we similarly implement a radiation boundary condition with a PML layer with a damping $\sigma = \sigma_2(z)$ see (24) below.

Denote

$$s_1(x) = \frac{i\omega}{\sigma_1(x) - i\omega}\,,$$

then, with the PMLs, the coupling transport equations can be written

$$\begin{aligned} &2ikA_z + s_1^2 A_{xx} + k^2\nu A + s_1 s_1' A_x \\ &\qquad = -(k^2\nu B + s_1^2 B_{xx} + s_1 s_1' B_x)e^{-2ikz}\,, \end{aligned} \tag{19}$$

$$\begin{aligned} &-2ikB_z + s_1^2 B_{xx} + k^2\nu B + s_1 s_1' B_x \\ &\qquad = -(k^2\nu A + s_1^2 A_{xx} + s_1 s_1' A_x)e^{2ikz}. \end{aligned} \tag{20}$$

With PML included we have the following two coupled parabolic approximations (with one lateral dimension):

$$2ikA_z + s_1^2 A_{xx} + k^2\nu A + s_1 s_1' A_x = -k^2\nu B e^{-2ikz}\,, \tag{21}$$

$$-2ikB_z + s_1^2 B_{xx} + k^2\nu B + s_1 s_1' B_x = -k^2\nu A e^{2ikz}. \tag{22}$$

At the boundary of the PML layer we use a zero dirichlet boundary condition.

3.3 P-H-D Iteration

In this section we describe in detail the iterative procedure we use to approximate the wave field. With the initial value $B^{(0)} = 0$, for each $m \geq 1$ we solve for $A^{(m)}$ and $u^{(m)}$ according to:

$$\left\{\begin{array}{rcl} 2ikA_z^{(m)} + s_1^2 A_{xx}^{(m)} + k^2\nu A^{(m)} + s_1 s_1' A_x^{(m)} &=& -k^2\nu B^{(m-1)} e^{-2ikz} \quad \text{in } \Omega_P \\ A^{(m)}(x,0) &=& \sqrt{k_0} e^{-\frac{|x|^2}{2}} - B^{(m-1)}(x,0) \end{array}\right. \tag{23}$$

$$\left\{\begin{array}{rcl} s_2\frac{\partial}{\partial z}(s_2\frac{\partial u^{(m)}}{\partial z}) + s_1\frac{\partial}{\partial x}(s_1\frac{\partial u^{(m)}}{\partial x}) + k^2(1+\nu)u^{(m)} &=& 0 \quad \text{in } \Omega_H, \\ iku^{(m)} + u_z^{(m)} &=& 2ikA^{(m)}e^{ikz} \quad \text{on } \Gamma, \\ u^{(m)} &=& 0 \quad \text{on } \partial\Omega_H\backslash\Gamma, \end{array}\right. \tag{24}$$

where $\sigma_1 = \sigma_1(x), \sigma_2 = \sigma_2(z)$ and $\sigma_1(x) > 0$ in the artificial domain giving damping of the plane wave modes in the lateral direction, $\sigma_2(z)$ giving damping of the wave in the propagation direction (at end of computational domain), whereas $\sigma_i = 0$ in the physical domain giving the Helmholtz equation there.

Then, having solved for $A^{(m)}$ and $u^{(m)}$ we compute $B^{(m)}$ by

$$\left\{\begin{array}{rcl} -2ikB_z^{(m)} + s_1^2 B_{xx}^{(m)} + k^2\nu B^{(m)} + s_1 s_1' B_x^{(m)} &=& -k^2\nu A^{(m)} e^{2ikz} \quad \text{in } \Omega_P \\ B^{(m)} &=& \frac{iku^{(m)} - u_z^{(m)}}{2ik} e^{ikz} \quad \text{on } \Gamma \end{array}\right. \tag{25}$$

This procedure generates $A^{(m)}$ in Ω_P, $u^{(m)}$ in Ω_H and $B^{(m)}$ in Ω_P sequentially. A simple modification of this procedure after the first iteration makes it parallel for $m \geq 2$.

$$\left\{\begin{array}{rcl} 2ikA_z^{(m)} + s_1^2 A_{xx}^{(m)} + k^2\nu A^{(m)} + s_1 s_1' A_x^{(m)} &=& -k^2\nu B^{(m-1)} e^{-2ikz} \quad \text{in } \Omega_P \\ A^{(m)}(x,0) &=& \sqrt{k_0} e^{-\frac{|x|^2}{2}} - B^{(m-1)}(x,0) \end{array}\right. \tag{26}$$

$$\left\{\begin{array}{rcl} s_2\frac{\partial}{\partial z}(s_2\frac{\partial u^{(m)}}{\partial z}) + s_1\frac{\partial}{\partial x}(s_1\frac{\partial u^{(m)}}{\partial x}) + k^2(1+\nu)u^{(m)} &=& 0 \quad \text{in } \Omega_H, \\ iku^{(m)} + u_z^{(m)} &=& 2ikA^{(m-1)} \quad \text{on } \Gamma, \\ u^{(m)} &=& 0 \quad \text{on } \partial\Omega_H\backslash\Gamma, \end{array}\right. \tag{27}$$

$$\left\{\begin{array}{rcl} -2ikB_z^{(m)} + s_1^2 B_{xx}^{(m)} + k^2\nu B^{(m)} + s_1 s_1' B_x^{(m)} &=& -k^2\nu A^{(m-1)} e^{2ikz} \quad \text{in } \Omega_P \\ B^{(m)} &=& \frac{iku^{(m-1)} - u_z^{(m-1)}}{2ik} e^{ikz} \quad \text{on } \Gamma. \end{array}\right. \tag{28}$$

3.4 Dispersion relation

Note that for Helmholtz homogeneous medium plane wave modes: $u = e^{i(k_x x + k_z z)}$, $k_x^2 + k_z^2 = k^2$ the interface conditions correspond to

$$\tilde{A} = \frac{iku + u_z}{2ik} e^{-ikz} = \frac{k + k_z}{2k} e^{i[k_x x + (k_z - k)z]},$$

$$\tilde{B} = \frac{iku - u_z}{2ik} e^{ikz} = \frac{k - k_z}{2k} e^{i[k_x x + (k_z + k)z]}.$$

The homogeneous medium parabolic approximation corresponds to the longitudinal wave number

$$\tilde{k}_z = k(1 - \frac{k_x^2}{2k^2}) = k\theta(k_x), \tag{29}$$

and modes of the form

$$A = e^{i[k_x x + (\tilde{k}_z - k)z]},$$

$$B = e^{i[k_x x + (\tilde{k}_z + k)z]}.$$

Hence, in the homogeneous case and with only modes traveling in the z direction with $k_x = 0$ the modes in the two domains coincide, but for general k_x they have a different representation.

4 Numerical Examples

Four different examples are presented in this section. We compare the PE and P-H solution with Helmholtz equation in the first three examples. In the last example, we show the PE and P-H solutions while we do not give the Helmholtz solution due to computer limitations. The experiments clearly show that our approach is much better in dealing with strong scattering than the PE method. Moreover, our approach produces comparable results to the full Helmholtz equation while having comparable cost to the PE method.

In the first three examples, the speed of propagation in the homogeneous medium is $330m/s$ and to the frequency being $25Hz$ so that the corresponding wavelength is

$13.2m$. In the discretization we use 6π grid points per wavelength in both directions. Our computational domain contains 400 grid points (horizontal) and 1400 grid-points (vertical), whereas on the left and the right sides, we use 15 grid points for the PML medium, and 50 grid points for PML medium in the propagation direction. The P-domain corresponds to the section from the source to 800 grid points while the rest comprises the H-domain.

4.1 Example 1

There is a single circular scatterer center at the 1000'th grid point (53 wavelengthes) from the source with a radius of 100 grid point (5 wavelengthes) in a homogeneous background medium with the speed of propagation in the scatterer being $467m/s$, faster than that of in the background medium.

In **Figure 2** the top left figure shows the speed of propagation in the medium. The background medium is homogeneous and there is one strong scatterer in the Helmholtz domain. The top right figure plots the reference solution for the magnitude of the wave field corresponding to solving the Helmholtz equation in the full domain. The two middle plots show the solution for the wave field obtained by using respectively the parabolic equation (PE) approximation and our P-H domain decomposition approach. Note that the PE solution does not capture well longitudinal scattering and is smooth whereas the P-H domain decomposition approach captures the high frequency components in the solution that is caused by such scattering events. In the two bottom plots we show the magnitude of the wave field evaluated at the center line corresponding to zero lateral offset. The solid lines correspond to the Helmholtz solution and the two dotted line to respectively the PE and the P-H domain decomposition solutions respectively.

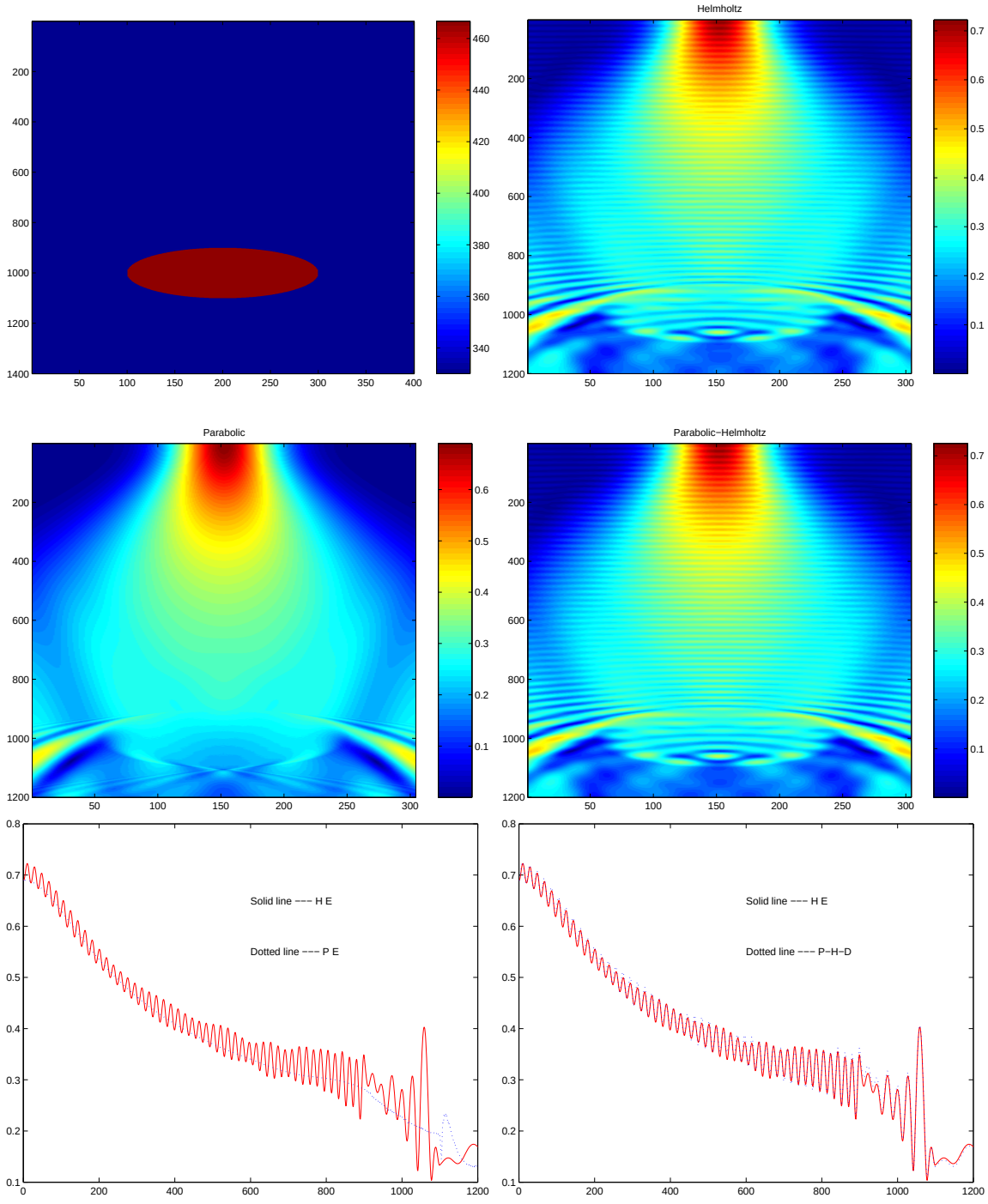

(a) Helmholtz and parabolic

(b) Helmholtz and P-H-D

Figure 2: The figure shows numerical approximations for the wave field using respectively the Helmholtz, the PE and the P-H domain decomposition methods when the medium contains a strong imbedded circular scatterer shown in the top left plot.

4.2 Example 2

In this example there are two identical scatterers that are located 1000 grid points (53 wavelengthes) away from source in the homogeneous medium. Each scatterer consists of two half circle and one rectangle. The speeds of propagation are $404m/s$ in the half circle and $466m/s$ in the rectangle respectively. The radius of the half circle is 40 grid points, the lengths of the rectangle's edges are 80 grid points and 120 grid points.

In **Figure 3** the top left figure shows the speed of propagation in the medium. The background medium is homogeneous and there are two strong scatterers in the Helmholtz domain. The top right figure plots the reference solution for the magnitude of the wave field corresponding to solving the Helmholtz equation in the full domain. The two middle plots show the solution for the wave field obtained by using respectively the parabolic equation (PE) approximation and our P-H domain decomposition approach. In the two bottom plots we show the magnitude of the wave field evaluated at the center line corresponding to zero lateral offset. The solid lines correspond to the Helmholtz solution and the two dotted line to respectively the PE and the P-H domain decomposition solutions.

4.3 Example 3

In this example we use the same circular scatterer as in Example one, but in this case we add also small random fluctuations in the bulk modulus. The (truncated) Gaussian random fluctuations correspond to the following model for the fluctuations ν: The correlation length in x-direction is 5, in z-direction is 10, and we use a Gaussian spectrum.

In **Figure 4** the top left figure shows the speed of propagation in the medium. The background medium is homogeneous and there is one strong scatterer in the Helmholtz domain. The speed of propagation now also contains a small modulating random component. The top right figure plots the reference solution for the

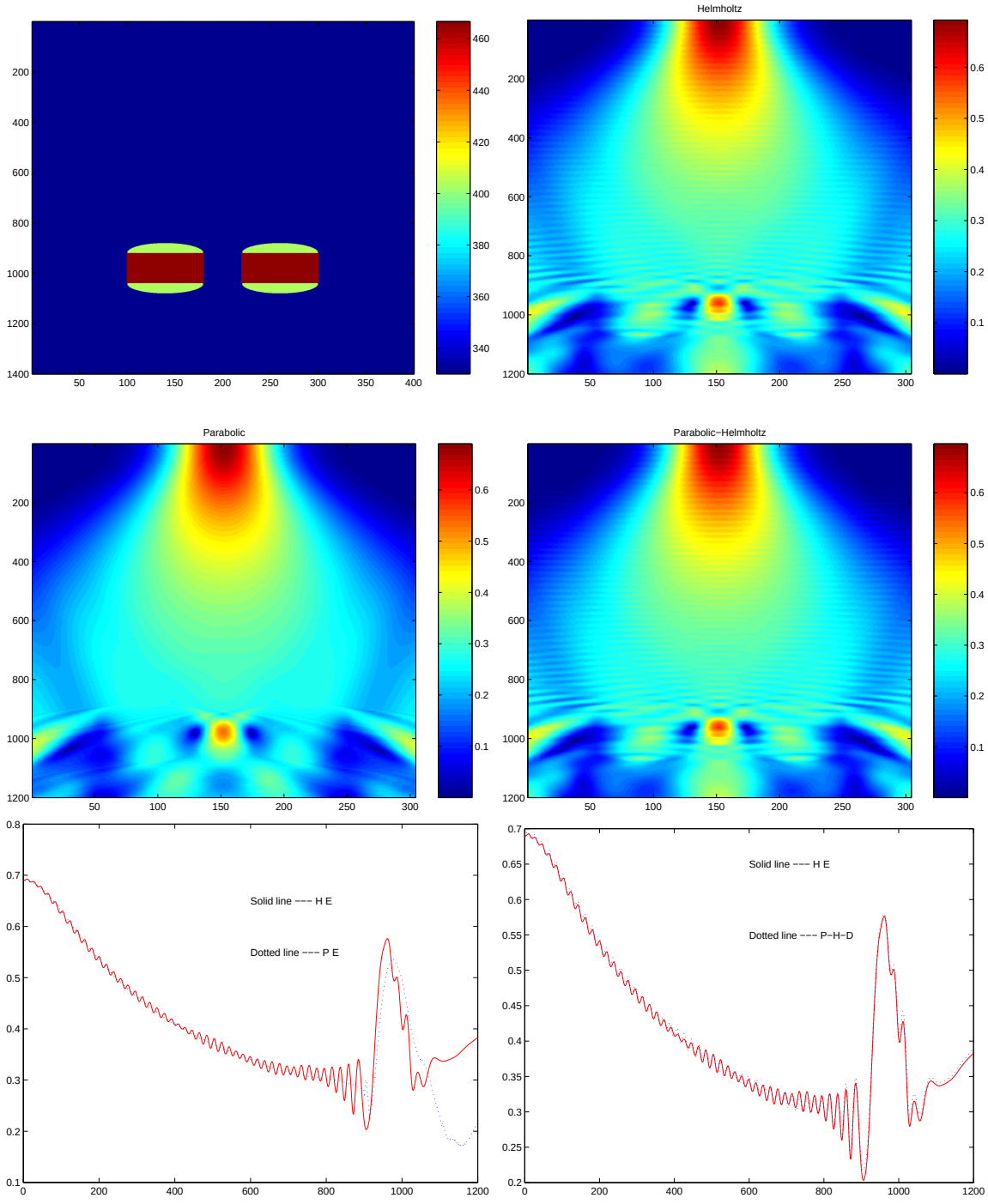

(a) Helmholtz and parabolic

(b) Helmholtz and P-H-D

Figure 3: The figure shows numerical approximations for the wave field using respectively the Helmholtz, the PE and the P-H domain decomposition methods when the medium contains two strong imbedded circular scatterers shown in the top left plot.

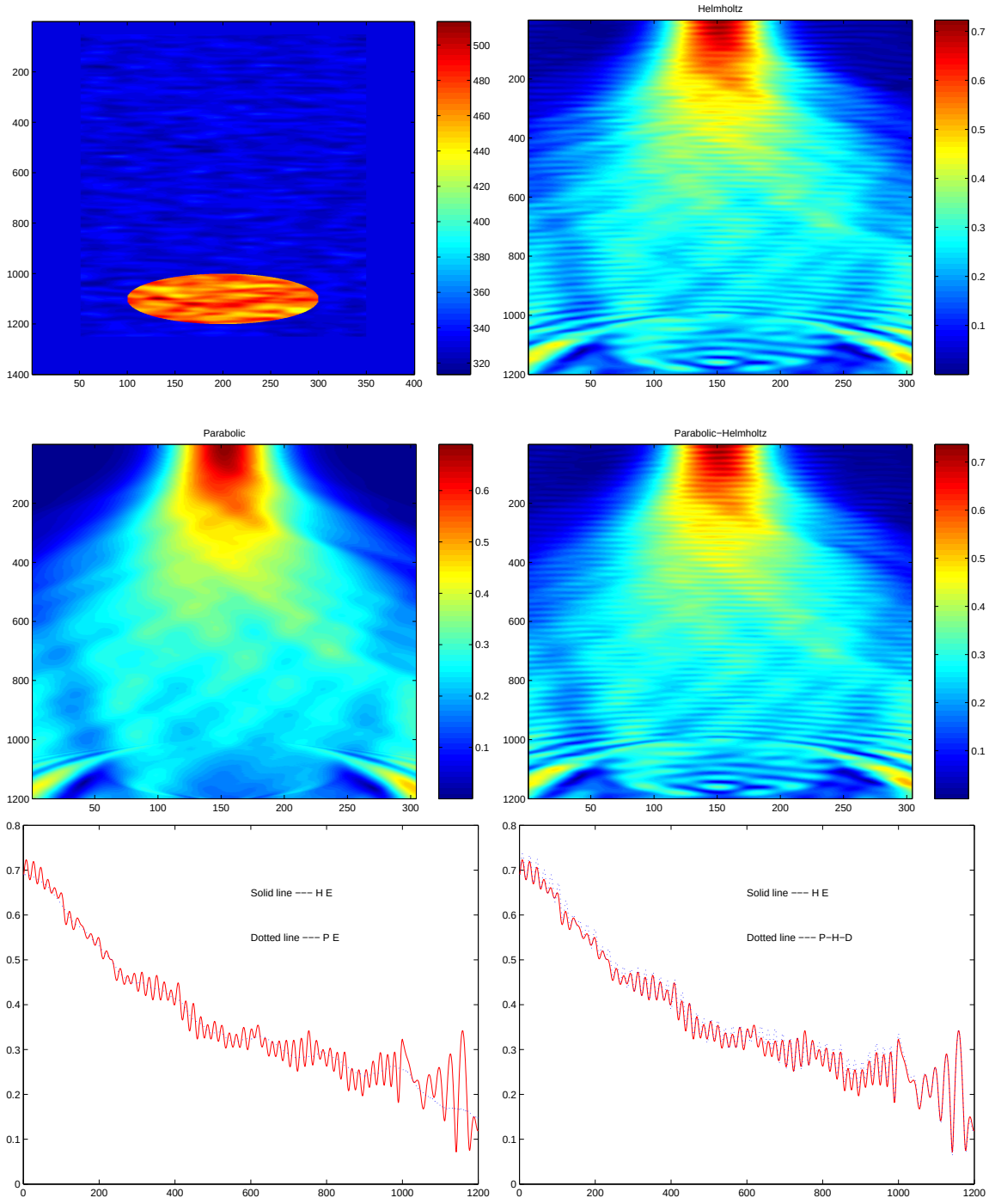

(a) Helmholtz and parabolic

(b) Helmholtz and P-H-D

Figure 4: The figure shows numerical approximations for the wave field using respectively the Helmholtz, the PE and the P-H domain decomposition methods when the medium contains a strong imbedded circular scatterer shown in the top left plot. In addition the medium contains modulating random fluctuations in the speed of propagation.

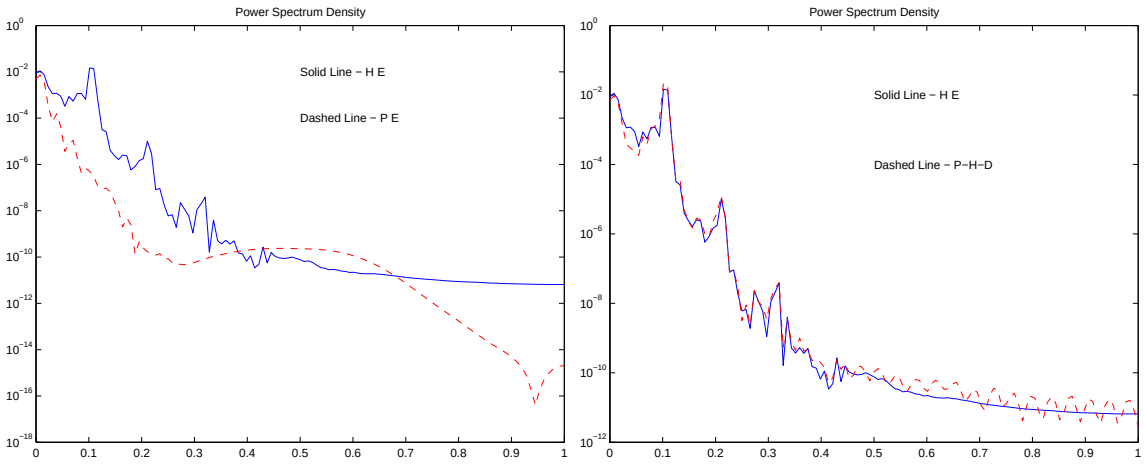

Figure 5: The Spectrum computed by different algorithms

magnitude of the wave field corresponding to solving the Helmholtz equation in the full domain. The two middle plots show the solution for the wave field obtained by using respectively the parabolic equation (PE) approximation and our P-H domain decomposition approach. Note that the PE solution does not capture well longitudinal scattering and is smooth whereas the P-H domain decomposition approach captures both the high frequency components in the solution that is caused by such scattering events and also the modification that is due to the accumulated effect of the small incoherent scatterers. In the two bottom plots we show the magnitude of the wave field evaluated at the center line corresponding to zero lateral offset. The solid lines correspond to the Helmholtz solution and the two dotted line to respectively the PE and the P-H domain decomposition solutions.

Figure 5 shows the spectrum for the signal trace corresponding to the center of the computational domain. Here we compute the spectrum as the Fourier transform of the modulus of the field. The solid line is the spectrum associated with the Helmholtz solver, while the dashed lines are the results of PE (a) and P-H-D (b) respectively. We see that the spectrum of the Helmholtz and P-H Domain decomposition solutions are very close.

4.4 Example 4

In this example, the computational domain contains $10,000$ grid-points (531 wavelengthes) in the propagation direction and 600 grid-points (32 wavelengthes) in horizontal direction. The frequency of the signal is $50Hz$, and the speed in the background medium is $1500m/s$. In the discretization, we use 6π points per wavelength. There is a single circular scatterer at the 9650'th grid-points (512 wavelengthes) away from the source and with 50 grid-points being the radius. The background medium is homogeneous and the speed of propagation in the scatterer is $2121m/s$, which is faster than that in the background medium. The domain from source to 9400 grid-points (499 wavelengthes) is our P-domain, the rest is the H-domain. The number of unknowns in the discretized linear system for Helmholtz equation then becomes 6 million.

In **Figure 6** the top figure shows the speed of propagation in the medium. The background medium is homogeneous and there is one strong scatterer in the Helmholtz domain. The two middle plots show the solution for the wave field obtained by using respectively the parabolic equation (PE) approximation and our P-H domain decomposition approach. In the two bottom plots we show the magnitude of the wave field evaluated at the center line corresponding to zero lateral offset. Again it shows that the PE approach can not capture the back scattering due to the presence of a strong scatterer. Also the discontinuity of the speed and the geometry of the scatterer boundary causes small oscillations due to dispersion errors in the PE approach.

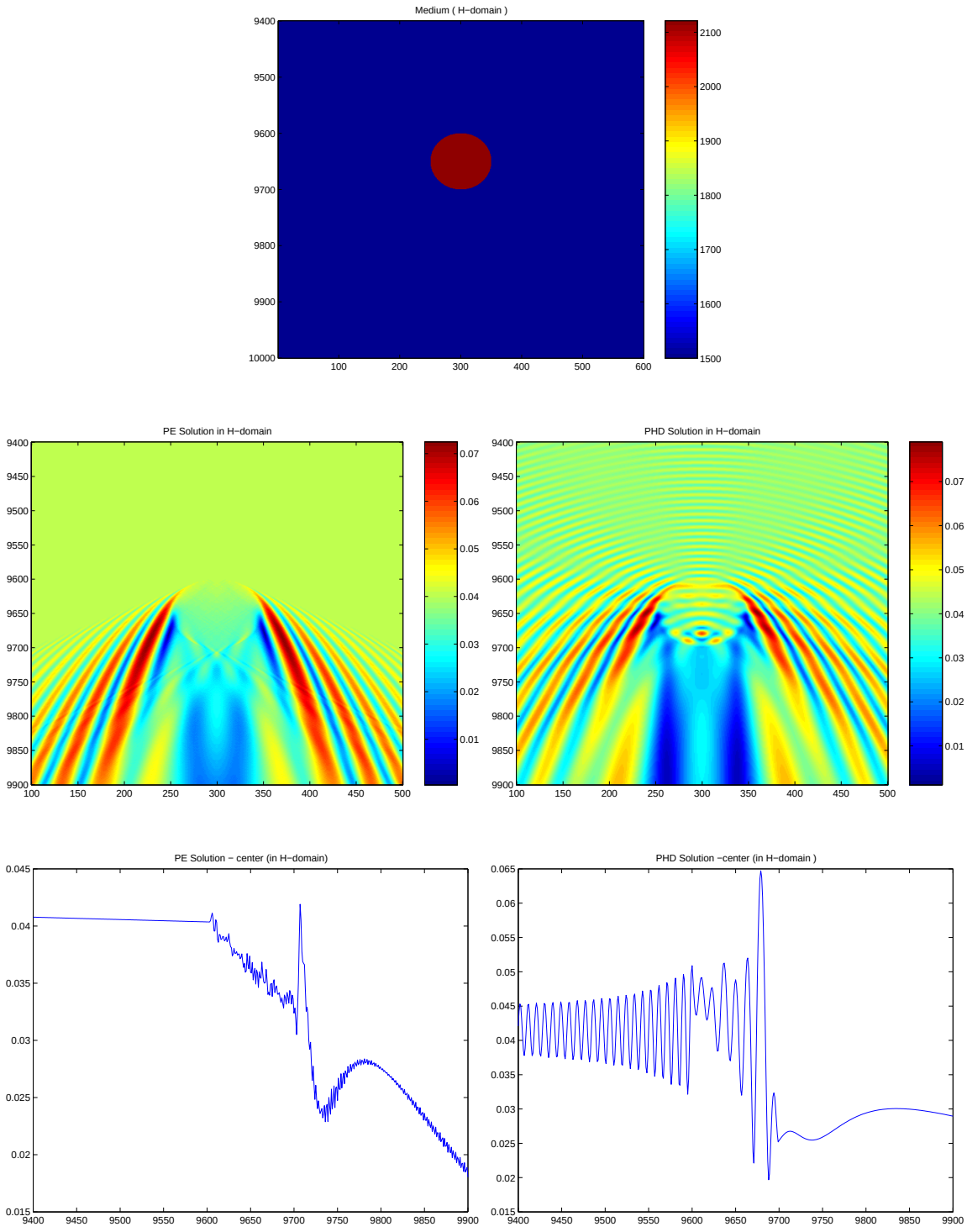

Figure 6: The figure shows numerical approximations for the wave field using respectively the PE and the P-H domain decomposition methods when the medium contains a strong imbedded circular scatterer shown in the above.

5 Conclusion

Our main motivation was to develop a numerical scheme that can handle strong scatterers on the one hand and long range propagation in a weakly fluctuating medium on the other. This has been accomplished by developing an algorithm that couples two different regimes of wave propagation: the parabolic and the Helmholtz regimes. We use a domain decomposition approach that divides the region into a parabolic and a Helmholtz domain. In the parabolic domain we decompose the wave field locally into forward and backward propagating modes. The domain decomposition and wave mode decomposition approach allows us to deal with long range wave propagation in the parabolic regime as well as strong scattering in the Helmholtz regime. Numerical examples demonstrate that our method is able to capture the effects of the strong scatterers that give strong coherent reflections as well as small scale fluctuations in the wave field that accumulate when the wave propagates over large distances.

Appendix A

Here we show the potential instability when solving the full system (11, 12) by iteration. We simplify the system by considering only one transverse variable x and the homogeneous case with $\nu = 0$. We then have

$$\begin{aligned} 2ikA_z + A_{xx} + B_{xx}e^{-2ikz} &= 0\,, \\ -2ikB_z + B_{xx} + A_{xx}e^{2ikz} &= 0. \end{aligned}$$

We analyze modes with lateral wave number k_x so that the mode iteration becomes

$$\begin{aligned} \mathcal{L}^+ A^{(m)} &= -B_{xx}^{(m-1)} e^{-2ikz}\,, \\ \mathcal{L}^- B^{(m)} &= -A_{xx}^{(m)} e^{2ikz}\,, \end{aligned} \tag{30}$$

where we defined the operators

$$\mathcal{L}^{\pm} = \pm 2ik\frac{\partial}{\partial z} + \frac{\partial^2}{\partial x^2}.$$

We apply the initial and boundary conditions

$$B^{(0)}(z,x) \equiv 0\,,$$
$$A^{(m)}(0,x) = a_0 e^{ik_x x} - B^{m-1}(0,x)\,, \quad B^{(m)}(L,x) = 0\,,$$

where L is the length of the considered slab and the end condition on the mode $B^{(m)}$ corresponds to a radiation condition. The eigenfunction modes satisfying $\mathcal{L}^{\pm}u^{\pm} = 0$ are

$$u^{\pm}(z,x) \;\; = \;\; e^{ik_x(x \mp k_x z/(2k))}.$$

We now consider the case with large wave numbers satisfying $k = k_x^2/(2k)$ corresponding to $\theta(k_x) = 0$ in (29). Then

$$u^{\pm}e^{\pm 2ikz} = u^{\mp}\,,$$

and the iteration (30) will in general exhibit rapid growth whereas modes with such lateral wave number are evanescent and rapidly decaying in the context of the Helmholtz equation.

We next show the growth by assuming

$$B^{(m-1)}(z,x) = b_0(L-z)^j e^{ik_x(x+zk_x/(2k))}\,, \quad A^{(m)}(0,x) = a_0 e^{ik_x x}.$$

Then, writing

$$A^{(m)}(z,x) \;\; = \;\; v(z)e^{ik_x x}\,,$$

we find when assuming $k = k_x^2/(2k)$

$$\frac{dv}{dz} + \frac{ik_x^2}{2k}v \;\; = \;\; -\frac{ik_x^2}{2k}(L-z)^j e^{-izk_x^2/(2k)}.$$

The rapid phase variation in the source term of this equation is canceled exactly by the phase variation of the propagator of the right hand side operator, that is, is canceled exactly by the integrating factor used in the solution of this equation. Thus,

the integral of the source term then becomes large for large lateral wave numbers k_x, we find explicitly:

$$\begin{aligned} A^{(m)}(z,x) &= \left(a_0 - ik_x b_0 \frac{L^{j+1} - (L-z)^{j+1}}{\sqrt{2}(j+1)}\right) e^{ik_x(x - k_x z/(2k))}, \\ B^{(m)}(z,x) &= -\left(ik_x a_0 \frac{L-z}{\sqrt{2}} + k_x^2 b_0 \frac{L^{j+1}(L-z)(j+2) - (L-z)^{j+2}}{2(j+1)(j+2)}\right) \\ &\quad \times e^{ik_x(x + k_x z/(2k))}. \end{aligned}$$

A similar, but slightly more complicated, analysis shows that there is a similar growth for *general* k_x since resonant modes are generated after several iterations. The rapid growth is caused by the coupling transverse Laplacian term, which is a lower order term in the parabolic regime. In heterogeneous media evanescent modes with specific lateral wave numbers can be generated by scattering. In numerical computations, roundoff errors or artificial boundary conditions can also generate such spurious evanescent modes and cause instability. Only if A and B are solved simultaneously with two appropriate point boundary conditions (which is the case for Helmholtz equation) are the evanescent modes under control. Due to this the iterative procedure for the coupled parabolic equations (11, 12) for A and B is numerically unstable when the coupling transverse Laplacian term is present.

References

[1] M. Ash, W.Kohler, G.C. Papanicolauou, M. Psotel and B. White, Frequency content of randomly scattered signals. SIAM Review, 33: 519-625, 1991.

[2] A. Bamberger, B. Engquist, L. Halpern and P. Joly, Parabolic wave equation approximations in heterogenous media. SIAM J. Appl. Math. 48 (1988), no. 1, 99–128.

[3] E.Becache, A.S.Bonnet-Ben Dhia and G.Legendre, Perfectly matched layers for the convected Helmholtz equation, SIAM J. Numer. Anal, Vol. 42, No. 1 pp 409-433.

[4] Jean-Pierre Berenger, A perfectly matched layer for the absorption of electromagnetic waves, Journal of computational physics 114, 185-200 (1994).

[5] X.C. Cai , M.A.Casarin, F.W.Elliott Jr. and O.B. Widlund, Overlapping Schwarz algorithms for solving Helmholtz's equation, in Domain decomposition methods, 10 (Boulder, CO, 1997), Amer. Math. Soc., Providence, RI 1998, P391-399.

[6] Francis Collino, Souad Ghanemi and Patrick Joly, Domain decomposition method for harmonic wave propagation: a general presentation, Comput. Methods Appl. Mech. Engrg. 184 (2000) 171-211.

[7] Michael D. Collins and Richard B. Evans, A two-way parabolic equation for acoustic backscattering in the ocean, J. Acoust. Soc. Am. 91(3) 1992, 1357-1368.

[8] J. F. Clouet and J. P. Fouque, Spreading of a pulse traveling in random media, Ann. Appl. Probab. **4** (1994), 1083-1097.

[9] M. V. de Hoop and A. K. Gautesen, Uniform asymptotic expansion of the square-root Helmholtz operator and the one-way wave propagator, SIAM J. Appl. Math., 63(3), 777-800, (2003).

[10] Ding Lee, William L. Siegman and Donald F. St. Mary, A numerical marching scheme to compute scattering in the ocean, mathematics and Computers in Simulation 34 (1992) 525-540.

[11] Ding Lee; Allan D. Pierce and Er-Chang SHANG, Parabolic Equation Development in the Twentieth Century, Journal of Computational Acoustics, Vol. 8, No. 4 (2000) pp 527-637.

[12] Finn B. Jensen, Willian A. Kuperman, Michael B. Porter and Henrik Schmidt, Computational Ocean Acoustics, AIP Press, 2nd ed. 2000.

[13] L. Fishman, One-way wave propatation methods in direct and inverse scalar wave propagation modeling, Radio Science 28, No. 5 (1993)

[14] L. Fishman, A.K. Gautesen and Z. Sun, Uniform high-frequency approximations of the square root Helmholtz operator symbol, Wave Motion 26 (1997) 127-161.

[15] K. Huang, K. Solna and H. Zhao, Coupled Parabolic Equations for Wave Propagation, to appear in Methods and Applications of Analysis.

[16] Y. Lu and J. McLaughlin, The Riccati method for the Helmholtz equation, J. Acoust. Soc. Am. 100(3), 1996.

[17] Y. Lu , One-way Large Range Step Methods for Helmholtz Waveguides, Journal of Computational Physics 152, 231-250 (1999).

[18] Y. Lu, Exact one-way methods for acoustic waveguides, Mathematics and computers in Simulation 50 (1999) 377-391.

[19] Erik M. Salomons, Computational atmospheric acoustics, Kluwer Academic Publishers, 2001.

[20] K. Solna, Stable Spreading of Acoustic Pulses due to laminated microstructure, Dissertation, Stanford University, 1997.

[21] K. Solna and G. C. Papanicolaou, Ray Theory for a Locally Layered Medium, Waves in Random Media, V 10, 151 - 198, 2000.

[22] F.D. Tappert, The parabolic approximation method, in *Wave Progpagation in Underwater Acoustics,* edited by J.B.Keller and J.S.Papadakis (Springer-Verlag, NewYork, 1977) pp. 224-287.